Non-Abelian phases in two-component ν=2/3 fractional quantum Hall states: Emergence of Fibonacci anyons

Zhao Liu, Abolhassan Vaezi, Kyungmin Lee, and Eun-Ah Kim

Phys. Rev. B **92**, 081102 — Published 5 August 2015

DOI: 10.1103/PhysRevB.92.081102

Non-Abelian phases in two-component $\nu = 2/3$ fractional quantum Hall states: Emergence of Fibonacci anyons

Zhao Liu,[1] Abolhassan Vaezi,[2,*] Kyungmin Lee,[2] and Eun-Ah Kim[2]

[1]*Department of Electrical Engineering, Princeton University, Princeton, New Jersey 08544, USA*
[2]*Department of Physics, Cornell University, Ithaca, New York 14853, USA*

Recent theoretical insights into the possibility of non-Abelian phases in $\nu = 2/3$ fractional quantum Hall (FQH) states revived the interest in the numerical phase diagram of the problem. In this letter, we investigate the effect of various kinds of two-body interlayer couplings on the (330) bilayer state and exactly solve the Hamiltonian for up to 14 electrons on sphere and torus geometries. We consider interlayer tunneling, short-ranged repulsive/attractive pseudo-potential interactions as well as Coulomb repulsion. We find 6-fold ground-state degeneracy on the torus when interlayer hollow-core interaction is dominant. To identify the topological nature of this phase we measure orbital-cut entanglement spectrum, quasi-hole counting, topological entanglement entropy and wave-function overlap. Comparing the numerical results to the theoretical predictions, we interpret this 6-fold ground-state degeneracy phase to be the non-Abelian bilayer Fibonacci state.

PACS numbers: 73.43.-f, 03.67.Lx, 05.30.Pr, 11.15.Yc

Introduction– There is a surging interest in the search for non-Abelian (NA) anyons in topological states of matter.[1–8] NA anyons register protected quantum memory and the stored information can be processed through braiding the world line of NA anyons. This comprises the basic notion of building fault tolerant quantum computers. Two famous examples are Ising and Fibonacci anyons which have been conjectured to emerge in $\nu = 5/2$ and $\nu = 12/5$ fractional quantum Hall (FQH) states, respectively.[9–11] In particular Fibonacci anyons are of interest for universal quantum computation. However, there is no experimental observation of these exotic quasiparticles in FQH systems to date. Another approach for realizing NA anyons is through coupling Abelian states via various types of interactions to drive phase transition to NA topological phases.[12–17] In a realistic experimental situation, some of the interactions considered in theoretical investigations are indeed relevant.[18–25] Pursuing this direction further can potentially lead to a novel venue for realizing NA anyons.

In this letter, we focus on the two-component FQH system at $\nu = 2/3$, whose parent state consists of two decoupled $\nu = 1/3$ Laughlin states. The two components may describe physical spins,[18] spatial (physical layer) degrees of freedom, e.g., in wide quantum well realization of $2/3$ state,[19–22] or valley indices in graphene-like systems.[23–25] For convenience, in this letter we refer to all these various realizations of two-component systems as "$2/3$ *bilayer*" state. Early studies of $2/3$ bilayer state focused on various possible Abelian phases[26] and experimental observation of phase transitions.[18,19] In particular McDonald and Haldane numerically established phase diagram of the system in presence of interlayer tunneling and bare Coulomb interaction projected to the lowest Landau level (LLL)[27] and confirmed possibility of various Abelian phases. Recent analytical insights into possibility of NA phases in $2/3$ bilayer state[3,28–33] brought this seemingly closed problem into new focus. However, results of Ref. 27 imply that microscopic realizations of these Abelian phases require perturbation to the model Hamiltonain consisting of interlayer tunneling and bare Coulomb interaction projected to the LLL. In fact such perturbations may already exist in experimental systems.

Therefore, the recent proposals[3,28–33] beg for revisiting the $2/3$ bilayer problem numerically considering modified interlayer Coulomb interaction and interlayer tunneling. Any two-body interaction projected to the LLL can be expanded in terms of the so-called Haldane pseudo-potentials, $\mathcal{V}_m$,[34,35] which are projector operators of two electrons to the state with relative angular momentum m. Modifying the Coulomb interaction amounts to changing the coefficient of the pseudo-potentials. Here, we modify the interlayer Coulomb interaction by changing its dominant components, namely $\mathcal{V}_0^{\text{inter}}$ and $\mathcal{V}_1^{\text{inter}}$ (also known as hollow-core interaction). We solve the resulting Hamiltonian for up to 14 electrons using exact diagonalization (ED) method and utilize a variety of numerical measurements to establish the nature of different topological phases achieved through varying coupling parameters. We obtain a wide range of parameters where enhancing $\mathcal{V}_1^{\text{inter}}$ and suppressing $\mathcal{V}_0^{\text{inter}}$ components of the Coulomb interaction drives phase transition to a NA state with Fibonacci anyons.

Model– We start with two $\nu = 1/3$ Laughlin states that are coupled through a number of distinct interlayer interactions. Let us now consider a torus with L_x, L_y dimensions. In the Landau gauge $\mathbf{A} = B(0, x)$, single particle states in the LLL are labeled by their momentum along y direction quantized as $k_y = 2\pi n/L_y$. The parent state, (330) Halperin state,[36] is the exact eigenstate of the following $\mathcal{V}_1$ Haldane's pseudo-potential $\mathcal{V}_1^{\text{intra}} = \sum_{\sigma=\uparrow,\downarrow}\sum_{n,r,s} V_{r,s}^{(1)} c_{n+r,\sigma}^\dagger c_{n+s,\sigma}^\dagger c_{n,\sigma} c_{n+r+s,\sigma}$, where $\sigma = \uparrow,\downarrow$ denotes the layer index, $c_{n,\sigma}$ annihilates an electron with $k_y = 2\pi n/L_y$ momentum, $V_{r,s}^{(1)} = \frac{\kappa^3}{\sqrt{2\pi}}\left(r^2 - s^2\right) e^{-\kappa^2 \frac{r^2+s^2}{2}}$, and $\kappa = 2\pi/L_y$.

We investigate the effects of interlayer coupling by considering both tunneling and interlayer two-body interaction of Haldane's $\mathcal{V}_0$ and $\mathcal{V}_1$ pseudo-potentials. The tunneling Hamiltonian is $\mathcal{H}_t = -t_\perp \sum_n c_n^\dagger \sigma_x c_n$, where $c_n^{\mathrm{T}} \equiv \left(c_{n,\uparrow}, c_{n,\downarrow}\right)$. The two-body interactions are $\mathcal{V}_0^{\text{inter}} = \sum_{\sigma;n,r,s} V_{r,s}^{(0)} c_{n+r,\sigma}^\dagger c_{n+s,-\sigma}^\dagger c_{n,-\sigma} c_{n+r+s,\sigma}$, where $V_{r,s}^{(0)} = \frac{\kappa}{\sqrt{2\pi}} e^{-\kappa^2 \frac{r^2+s^2}{2}}$ and $\mathcal{V}_1^{\text{inter}} = \sum_{\sigma;n,r,s} V_{r,s}^{(1)} c_{n+r,\sigma}^\dagger c_{n+s,-\sigma}^\dagger c_{n,-\sigma} c_{n+r+s,\sigma}$. In order to

Phase	c	GSD	$\mathcal{S}$	$\mathcal{D}$	OES
(330)	2	9	3	3	$1,2,5,10,20,\cdots$
$\overline{1/3}$	0	3	0	$\sqrt{3}$	$1,1,2,3,5,\cdots$
(112)	0	3	1	$\sqrt{3}$	
Fibonacci	$14/5$	6	3	$\sqrt{\frac{3}{2}\left(5+\sqrt{5}\right)}$	$1,1,3,6,13,\cdots$
I. L. Pfaffian	$5/2$	9	3	$\sqrt{12}$	$1,2,6,13,\cdots$
Z_4 RR	2	15	3	6	$1,1,3,6,13,\cdots$

Table I. Total central charge c, ground-state degeneracy (GSD), the sphere shift $\mathcal{S} = \nu^{-1}N_e - N_\Phi$, total quantum dimension $\mathcal{D}$, and orbital-cut entanglement spectrum (OES) counting for $l = 0,1,2,3,4,\cdots$ (l is the angular momenta relative to the ground state) for various topological phases at $\nu = 2/3$. For NA states, the OES counting generally depends on the number of electrons N_e^A and the pseudospin S_z^A in region A. Here we only show the case when $N_e^A/2$ ($N_e^A/4$) is an integer and $S_z^A = 0$ for the Fibonacci and I. L. Pfaffian states (Z_4 RR state). Although the counting of the bilayer Fibonacci state with $N_e^A = 0$ (mod 2) and Z_4 RR state with $N_e^A = 0$ (mod 4) are equal for $l \leq 4$, they are different for other values of N_e^A. The counting of the (112) state is the convolution of the counting of two counter-propagating $U(1)$ modes.

address the stability of the phases we obtain with this model we also consider the effect of interlayer Coulomb interaction in the limit of negligible interlayer separation perturbed by the above terms.

Candidate phases– Below, we consider two categories of possible states at $\nu = 2/3$: Abelian and non-Abelian, each with three members. Tables I summarizes some of their defining properties. *(i)* (330) *state* which is simply two decoupled $\nu = 1/3$ Laughlin states. This phase has 9-fold degenerate ground states on the torus. *(ii)* $\overline{1/3}$*: Particle-hole(PH) conjugate of the* $\nu = 1/3$ *Laughlin state*.[37,38] *(iii) Layer singlet state: non-chiral* (112) *Halperin state*.[36–39] *(iv) Bilayer Fibonacci phase*[3], which is a non-Abelian state described by $SU(3)_2$ Chern-Simons field theory and contains 6 distinct quasiparticles, three of which are non-Abelian with $d = \frac{1+\sqrt{5}}{2}$ quantum dimension. *(v) Interlayer (I. L.) Pfaffian state*,[32] which has 9 distinct quasiparticles and its wavefunction can be written as the product of (221) Halperin state and a Pfaffian wave-function.[32] *(vi) Fermionic* $(M = 1)$ Z_4 *Read-Rezayi (RR) state*.[28,29,40] This non-Abelian state with 15 distinct quasiparticles is described by $Z_4 \times U(1)_6$ edge conformal field theory. A unique feature of this state is the emergence of a non-Abelian quasihole excitation with $-e/6$ fractional charge.

Numerical results– Now we numerically search for possible phases by exact diagonalization of our model Hamiltonian. To mitigate the limitations of finite-size system study, we make measurements of various characteristics of topological phases using both toroidal and spherical geometries. The number of electrons N_e and total number of quantum fluxes N_Φ are related through $N_\Phi = \frac{3}{2}N_e$ relation on the torus and on the sphere $N_\Phi = \frac{3}{2}N_e - \mathcal{S}$, where $\mathcal{S}$ is the shift of a FQH state on sphere.[41] Good quantum numbers that can be used to label energy states are the total center-of-mass momentum K on the torus and angular momentum L_z on the sphere. In the absence of the interlayer tunneling, the total pseudospin

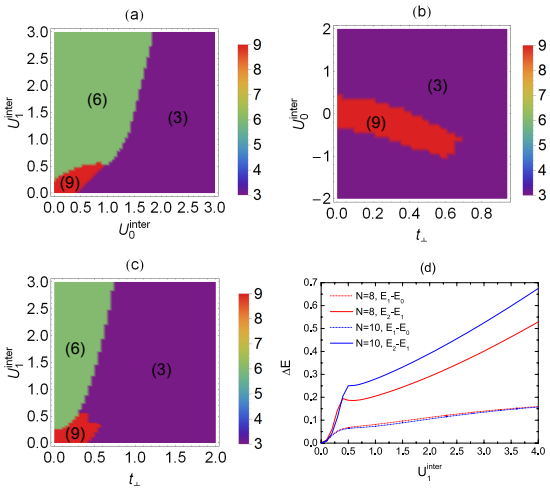

Figure 1. (Color online) The phase diagram based on GSD of the Hamiltonian $H = \mathcal{V}_1^{\text{intra}} + U_0^{\text{inter}}\mathcal{V}_0^{\text{inter}} + U_1^{\text{inter}}\mathcal{V}_1^{\text{inter}} + \mathcal{H}_t$. The numbers in the parentheses indicate GSD. (a)-(c) The GSD for $N_e = 8$ particles for (a) $t_\perp = 0$, (b) $U_1^{\text{inter}} = 0$, and (c) $U_0^{\text{inter}} = 0$. (d) The GSD as a function of U_1^{inter} for $N_e = 8$ and 10 electrons with $U_0^{\text{inter}} = t_\perp = 0$. E_0, E_1, E_2 are the lowest three energy levels in the $K < N_\Phi/3$ sectors. One can see that with the increase of U_1^{inter}, $E_2 - E_1 \gg E_1 - E_0$, implying a total 6-fold degeneracy.

$S_z = \frac{1}{2}(N_\uparrow - N_\downarrow)$ is also a good quantum number, where $N_{\uparrow,(\downarrow)}$ is the electron number in the upper (lower) layer.

Below we present the resulting phase diagram and the measurements characterizing the phases.

(a) Ground-state degeneracy: The GSD on the torus is significant as it equals the number of distinct anyon excitations.[42] Fig. 1 shows the phase diagram of the interaction $H = \mathcal{V}_1^{\text{intra}} + U_0^{\text{inter}}\mathcal{V}_0^{\text{inter}} + U_1^{\text{inter}}\mathcal{V}_1^{\text{inter}} + \mathcal{H}_t$ exhibiting several phases with 3-fold (purple), 6-fold (green), and 9-fold (red) GSD phases. Of these the 9-fold GSD region in Figs. 1(a) and (b) is smoothly connected to the parent state, so it is most likely the (330) phase. For the 3-fold GSD region, there are two Abelian candidates (see Table I) which can be differentiated by their different shifts on sphere, $\mathcal{S}$. The most tantalizing is the 6-fold GSD region, for which the NA bilayer Fibonacci state is the only candidate to the best of our knowledge. Figs. 1(a)-(c) show that dominant $\mathcal{V}_1^{\text{inter}}$ is required for the 6-fold GSD phase. Nevertheless, this phase is stable against subdominant tunneling and $\mathcal{V}_0^{\text{inter}}$ terms. In the rest of this letter, we will focus on the $t_\perp = 0$ limit where we can take advantage of S_z as a good quantum number. Fig. 1(d) shows that this degeneracy is stable upon increasing the system size.

To further address the stability of the 6-fold GSD phase against higher order pseudo-potentials which must exist in any realistic setting, we study $H = H_{\text{coulomb}}^{\text{intra}} + H_{\text{coulomb}}^{\text{inter}} + U_0^{\text{inter}}\mathcal{V}_0^{\text{inter}} + U_1^{\text{inter}}\mathcal{V}_1^{\text{inter}}$ Hamiltonian with $U_0^{\text{inter}} < 0$. We consider this particular form, because the $\mathcal{V}_0^{\text{inter}}$ component of the bare Coulomb interaction is larger than its $\mathcal{V}_1^{\text{inter}}$ component. Intriguingly, Fig. 2(a) shows that this Hamiltonian can stabilize the 6-fold GSD phase with a robust degeneracy and a large gap. Moreover, the finite-size scaling of the energy gap and the ground-state splitting [Fig. 2(b)] shows that this phase

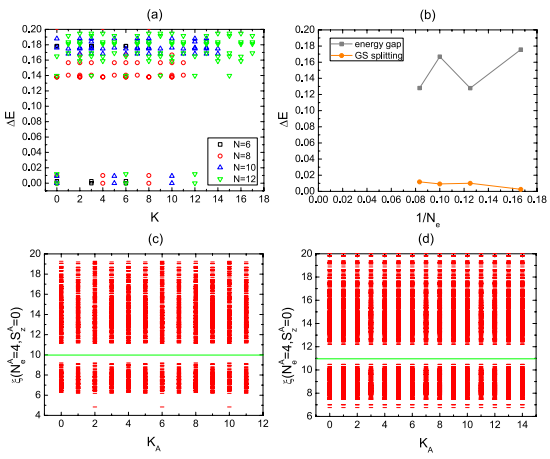

Figure 2. (Color online) Here we consider the interaction $H^{\text{intra}}_{\text{coulomb}} + H^{\text{inter}}_{\text{coulomb}} + U_0^{\text{inter}}\mathcal{V}_0^{\text{inter}} + U_1^{\text{inter}}\mathcal{V}_1^{\text{inter}}$ with $U_0^{\text{inter}} = -0.4$ and $U_1^{\text{inter}} = 0.6$ on the square torus.[43] (a) The energy spectrum of $N_e = 6, 8, 10$ and 12 electrons in the $S_z = 0$ sector. (b) The finite-size scaling of the energy gap and the ground-state splitting in the $S_z = 0$ sector. (c) The PES of $N_e = 8$ electrons, the counting below the gap (green line) is 1332. (d) The PES of $N_e = 10$ electrons, the counting below the gap (green line) is 4875.

is probably gapped in the thermodynamic limit. The finite-size scaling of the energy gap on the sphere also supports this conclusion [Fig. 3(c)].

(b) Edge state counting and entanglement spectrum: Orbital-cut entanglement spectrum (OES)[44] encodes the degeneracy of the edge excitations with angular momentum l relative to the ground-state.[39] We computes the OES on the sphere which leads to a single boundary. For a bilayer FQH system without interlayer tunneling, each OES level on the sphere can be labeled by the total electron number N_e^A, the total angular momentum L_z^A and the total pseudospin S_z^A in the subregion A.

Table I lists the expected counting for the candidate phases that can be obtained using the thin torus patterns and generalized exclusion rules.[45,55] Care has to be given to the fact that OES counting generally depends on N_e^A. For example, in the case of Abelian phases, OES is independent of N_e^A, while for the bilayer Fibonacci state it depends on the parity of N_e^A. In the case of Z_4 RR state, the counting depends on N_e^A modulo 4. In general, it can be shown that the OES counting of a $k-$electron clustered topological phase described by $SU(n)_k$ Chern-Simons theory depends on N_e^A modulo k. For the bilayer Fibonacci state, the counting for $N_e^A = 2M + 1$ is $1, 2, 5, 10, \cdots$. For the Z_4 RR state, the counting is $1, 2, 5, 10, \cdots$ $(1, 2, 6, 11, \cdots)$ for $N_e^A = 4M - 1$ ($N_e^A = 4M - 2$) for large values of N_e^A. For finite systems, the counting is slightly different. For instance, when $N_e = 6$ the expected counting for the bilayer Fibonacci (Z_4 RR) state is $1, 1, 3, 6, 12, \cdots$ $(1, 2, 5, 7, \cdots)$. For $N_e^A = 7$, the expected counting of the Z_4 RR state becomes $1, 2, 4, 7, \cdots$.

For the region with 9-fold GSD we obtained OES counting consistent with Abelian (330) state: $1, 2, 5, 10, 20, \cdots$ independent of N_e^A. On the other hand, the measured OES counting for the 6-fold GSD phase is different for the odd and even values of N_e^A, and distinct from any Abelian state. The OES counting of the modified interlayer Coulomb interaction with 6-fold GSD is presented in Figs. 3(a)-(b). The OES counting we obtain for the bilayer Fibonacci state dictates the following generalized Pauli exclusion rules: (a) In every three consecutive orbitals, there are at most two electrons. (b) Each configuration of two electrons with distance more than two orbitals such as (1001) or (10001) is doubly degenerate after assigning spin indices and must be counted twice. It was shown that these rules give rise to 6-fold GSD on the torus, and result in three NA anyon excitations with $d = \frac{1+\sqrt{5}}{2}$ quantum dimension, hence the Fibonacci anyons.[3]

The fact that the counting for $l = 1$ is unambiguously 1 for $N_e^A = 6$ rules out the I. L. Pfaffian and Z_4 RR states (for both of these states at $l = 1$, we expect the counting to be 2). Moreover, the fact that the measured OES counting depends on the parity of N_e^A indicates that the 6-fold GSD phase is a paired state with $k = 2$. This is consistent with the $SU(3)_2$ Chern-Simons description of the bilayer Fibonacci state.

(c) quasihole counting: The degeneracy of the ground-state in the presence of quasihole excitations, usually referred to as quasihole counting, is a telling property of a topological phase.[46,47] One way to create quasiholes is by adding additional fluxes to the system. For instance, in the bilayer Fibonacci phase, each additional flux would create two quasiholes. Another way is to use particle-cut entanglement spectrum (PES) which is achieved by tracing out some electrons in the density matrix associated with the ground-state wave function.[48] Each PES level is labeled by the total electron number N_e^A, momentum K_A and pseudospin S_z^A in the subsystem A. In Figs. 2(c) and (d), we observe a clear gap in the PES. The counting below gap is different from the expected counting for the Abelian as well as I. L. Paffian and Z_4 RR states,[55] while it is consistent with the generalized Pauli exclusion rules of the bilayer Fibonacci state described in the previous section.

(d) Topological entanglement entropy (TEE): The entanglement entropy of a two-dimensional gapped state follows $S_A(L) = \alpha L - \gamma$ relation, where L is the perimeter of subregion A. The sub-leading constant γ is related to the total quantum dimension of the topological phase $\mathcal{D}$, through $\gamma = \log \mathcal{D}$[49,50] relation. The precise numerical evaluation of the TEE for small systems is usually challenging.[51–54] However, qualitative aspects of our results in Fig. 3(d) are suggestive of 6-fold GSD phase is a NA state. The numerically estimated γ for the 6-fold GSD state is larger than the estimated γ for the unperturbed (330) state and far from the values of γ for the remaining Abelian phases whose γ's are expected to be half the value of (330) state (see Table I). Although this argument suggests the resulting state is NA, it does not rule out the possibility of other NA states.

(e) Wave-function overlap: We have also computed the squared overlap of the ground state of the 6-fold GSD region on the sphere with several candidate states in Table I. The overlap with the (112), $\overline{1/3}$ and Z_4 RR state is always negligible. The overlap with the (330) state is only 0.12 for 12 electrons. The overlap with the I. L. Pfaffian state is 0.80 for

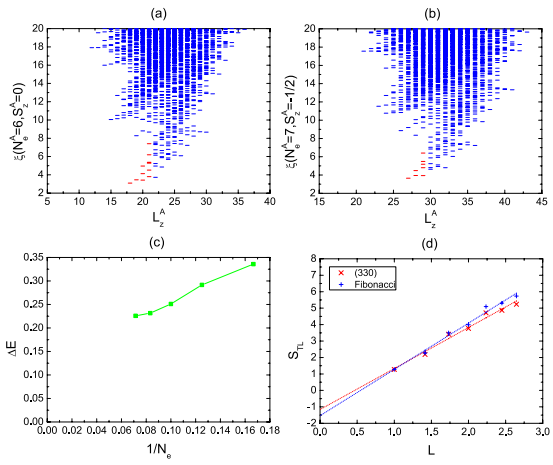

Figure 3. (Color online) For (a)-(c) we consider the modifies Coulomb interaction with $H^{\text{intra}}_{\text{coulomb}} + H^{\text{inter}}_{\text{coulomb}} + U_0^{\text{inter}}\mathcal{V}_0^{\text{inter}} + U_1^{\text{inter}}\mathcal{V}_1^{\text{inter}}$ with $U_0^{\text{inter}} = -0.4$ and $U_1^{\text{inter}} = 0.6$ on the sphere. (a) and (b) show the OES for $N_e = 14$ electrons in the $N_e^A = 6, S_z^A = 0$ and $N_e^A = 7, S_z^A = -1/2$ sectors. The levels consistent with the exclusion rule proposed in the text are colored by red. (c) The finite-size scaling of the energy gap in the $S_z = 0$ sector. (d) The measured entanglement entropy $S_A(L)$ for different boundary lengths, L, and its extrapolation using the method in Ref.[51] for the unperturbed (330) state and the 6-fold GSD phase in the large $\mathcal{V}_1^{\text{inter}}$ limit.

8 electrons, which is not quite low, but it decays very quickly to 0.73 and 0.66 when the system increases to 10 and 12 electrons.

To gain analytical insight about the numerical results, we also studied the thin torus limit of the coupled (330) system.[55] We show that at least four of the topological phases conjectured in Table I are plausible. Further, we obtain the thin torus patterns of the ground states.[56–59] We then use the resulting patterns to extract several key information about the nature of the underlying topological order, e.g. GSD, fusion rules and quantum dimensions of the anyons.[3,58] In particular we confirmed that the numerically obtained ground-states of the 6-fold GSD phase in the thin torus limit are consistent with the thin torus patterns of the bilayer Fibonacci state.[55]

Discussion– In summary, we reinvestigated the phase diagram of the coupled (330) bilayer state and considered the effects of modified interlayer Coulomb interaction by varying its $\mathcal{V}_0^{\text{inter}}$ and $\mathcal{V}_1^{\text{inter}}$ components. We have verified the result of McDonald and Haldane[27] indicating that interlayer tunneling and bare Coulomb interaction projected to the LLL can only yield Abelian phases. However, we found that when the pseudopotential components decay smoothly and both $g_1 \equiv \mathcal{V}_1^{\text{inter}}/\mathcal{V}_1^{\text{intra}}$ and $g_2 \equiv \mathcal{V}_1^{\text{inter}}/\mathcal{V}_0^{\text{inter}}$ increase, the resulting ground-state exhibits many properties of the bilayer Fibonacci phase. To the best of our knowledge this is the first numerical evidence for topological quantum phase transition between (330) state and a NA phase. Moreover the robustness of the bilayer Fibonacci phase which contains Fibonacci anyons which are capable of performing universal quantum computation is tantalizing.

Our result raises the question of how 6-fold GSD region of our model can be realized experimentally. Our calculations indicate that when g_1 and g_2 ratios are large enough, the Fibonacci state becomes energetically favorable. If the interlayer distance is small, $\mathcal{V}_1^{\text{inter}} \approx \mathcal{V}_1^{\text{intra}}$ so $g_1 \approx 1$. One strategy to get larger g_2 is to go to higher Landau levels with $2/3$ filling.[60,61] It is known that in higher Landau levels, $\mathcal{V}_0$ component of the bare Coulomb interaction decreases w.r.t. LLL while other components do not change too much. Although in the second Landau level (2LL) for 2DEG systems, $g_2 \approx 0.68$ is significantly larger than its value 0.5 in the LLL, unfortunately we do not have smooth pseudopotentials (the $\mathcal{V}_2$ component is larger than the $\mathcal{V}_1$ component). However, in the 2LL for graphene-like systems, $g_2 \approx 0.70$ grows and pseudopotentials decay smoothly. In fact, it can be shown through ED that even the bare Coulomb interlayer interaction projected to the 2LL in graphene yields a 6-fold degenerate ground-state in the $S_z = 0$ sector, and considering slight finite interlayer distance stabilizes that phase even further.[62] Therefore, we expect that graphene is a promising platform for the Fibonacci state.

Acknowledements– Authors acknowledge very useful discussions with Nicolas Regnault and Stefanos Kourtis. Z. Liu was supported by the Department of Energy, Office of Basic Energy Sciences through Grant No. DE-SC0002140. A. Vaezi, K. Lee, and E.-A. Kim were supported by NSF CAREER DMR-0955822. After the completion of this work, we became aware of related works in Refs. 63–65.

* vaezi@cornell.edu

1 C. Nayak, S. H. Simon, A. Stern, M. Freedman, and S. Das Sarma, Rev. Mod. Phys. **80**, 1083 (2008).
2 J. Alicea, Rep. Progress Phys. **75**, 076501 (2012).
3 A. Vaezi and M. Barkeshli, Phys. Rev. Lett. **113**, 236804 (2014).
4 N. H. Lindner, E. Berg, G. Refael, and A. Stern, Phys. Rev. X **2**, 041002 (2012).
5 D. J. Clarke, J. Alicea, and K. Shtengel, Nature Comm. **4**, 1348 (2013).
6 M. Cheng, Phys. Rev. B **86**, 195126 (2012).
7 A. Vaezi, Phys. Rev. B **87**, 035132 (2013).
8 M. Barkeshli, C.-M. Jian, and X.-L. Qi, Phys. Rev. B **88**, 241103(R) (2013).
9 G. Moore and N. Read, Nuclear Physics B **360**, 362 (1991).
10 X. G. Wen, Phys. Rev. Lett. **66**, 802 (1991).
11 N. Read and E. Rezayi, Phys. Rev. B **59**, 8084 (1999).
12 E. Ardonne and K. Schoutens, Phys. Rev. Lett. **82**, 5096 (1999).
13 A. Cappelli, L. S. Georgiev, and I. T. Todorov, Nuclear Physics B **599**, 499 (2001).
14 X.-G. Wen, Phys. Rev. Lett. **84**, 3950 (2000).
15 E. Fradkin, C. Nayak, and K. Schoutens, Nuclear Physics B **546**, 711 (1999).
16 Z. Papić, M. O. Goerbig, N. Regnault, and M. V. Milovanović, Phys. Rev. B **82**, 075302 (2010).

[17] M. R. Peterson and S. Das Sarma, Phys. Rev. B **81**, 165304 (2010).
[18] J. P. Eisenstein, H. L. Stormer, L. N. Pfeiffer, and K. W. West, Phys. Rev. B **41**, 7910 (1990).
[19] Y. W. Suen, H. C. Manoharan, X. Ying, M. B. Santos, and M. Shayegan, Phys. Rev. Lett. **72**, 3405 (1994).
[20] H. C. Manoharan, Y. W. Suen, M. B. Santos, and M. Shayegan, Phys. Rev. Lett. **77**, 1813 (1996).
[21] T. S. Lay, T. Jungwirth, L. Smrčka, and M. Shayegan, Phys. Rev. B **56**, R7092 (1997).
[22] J. Shabani, Y. Liu, and M. Shayegan, Phys. Rev. Lett. **105**, 246805 (2010).
[23] X. Du, I. Skachko, F. Duerr, A. Luican, and E. Y. Andrei, Nature (London) **462**, 192 (2009).
[24] K. I. Bolotin, F. Ghahari, M. D. Shulman, H. L. Stormer, and P. Kim, Nature (London) **462**, 196 (2009).
[25] C. R. Dean, A. F. Young, P. Cadden-Zimansky, L. Wang, H. Ren, K. Watanabe, T. Taniguchi, P. Kim, J. Hone, and K. L. Shepard, Nature Physics **7**, 693 (2011).
[26] B. I. Halperin, Helv. Phys. Acta **56**, 75 (1983).
[27] I. A. McDonald and F. D. M. Haldane, Phys. Rev. B **53**, 15845 (1996).
[28] E. Rezayi, X.-G. Wen, and N. Read, arXiv:1007.2022.
[29] M. Barkeshli and X.-G. Wen, Phys. Rev. Lett. **105**, 216804 (2010).
[30] A. Vaezi, Phys. Rev. X **4**, 031009 (2014).
[31] R. S. Mong, D. J. Clarke, J. Alicea, N. H. Lindner, P. Fendley, C. Nayak, Y. Oreg, A. Stern, E. Berg, K. Shtengel, and M. P. Fisher, Phys. Rev. X **4**, 011036 (2014).
[32] E. Ardonne, F. J. M. v. Lankvelt, A. W. W. Ludwig, and K. Schoutens, Phys. Rev. B **65**, 041305 (2002).
[33] P. Bonderson and J. K. Slingerland, Phys. Rev. B **78**, 125323 (2008).
[34] F. D. M. Haldane, Phys. Rev. Lett. **51**, 605 (1983).
[35] S. C. Davenport and S. H. Simon, Phys. Rev. B **85**, 075430 (2012).
[36] B. I. Halperin, Phys. Rev. Lett. **52**, 1583 (1984).
[37] J. K. Jain, Phys. Rev. Lett. **63**, 199 (1989).
[38] J. K. Jain, *Composite Fermions, by Jainendra K. Jain, Cambridge, UK: Cambridge University Press, 2007* (2007).
[39] X.-G. Wen, *Quantum Field Theory of Many-Body Systems* (Oxford Univ. Press, Oxford, 2004).
[40] C. H. Lee, Z. Papić, and R. Thomale, arXiv:1502.04663.
[41] X. G. Wen and A. Zee, Phys. Rev. Lett. **69**, 953 (1992).
[42] X. G. Wen and A. Zee, Phys. Rev. B **46**, 2290 (1992).
[43] These parameters are chosen to make the ground states deeply in the 6-fold degeneracy region. $U_0^{\text{inter}} = -0.4, U_1^{\text{inter}} \gtrsim 0.3$ is already enough to get qualitatively the same results.
[44] H. Li and F. D. M. Haldane, Phys. Rev. Lett. **101**, 010504 (2008).
[45] B. A. Bernevig and F. D. M. Haldane, Phys. Rev. Lett. **100**, 246802 (2008).
[46] N. Read and E. Rezayi, Phys. Rev. B **54**, 16864 (1996).
[47] S. H. Simon, E. H. Rezayi, N. R. Cooper, and I. Berdnikov, Phys. Rev. B **75**, 075317 (2007).
[48] A. Sterdyniak, N. Regnault, and B. A. Bernevig, Phys. Rev. Lett. **106**, 100405 (2011).
[49] A. Kitaev and J. Preskill, Phys. Rev. Lett. **96**, 110404 (2006).
[50] M. Levin and X.-G. Wen, Phys. Rev. Lett. **96**, 110405 (2006).
[51] M. Haque, O. Zozulya, and K. Schoutens, Phys. Rev. Lett. **98**, 060401 (2007).
[52] O. S. Zozulya, M. Haque, K. Schoutens, and E. H. Rezayi, Phys. Rev. B **76**, 125310 (2007).
[53] A. M. Läuchli, E. J. Bergholtz, and M. Haque, New J. Phys. **12**, 075004 (2010).
[54] Z. Liu, E. J. Bergholtz, H. Fan, and A. M. Läuchli, Phys. Rev. B **85**, 045119 (2012).
[55] *See the Supplemental Material.*
[56] E. J. Bergholtz and A. Karlhede, Journal of Statistical Mechanics: Theory and Experiment **2006**, L04001 (2006).
[57] A. Seidel and D.-H. Lee, Phys. Rev. Lett. **97**, 056804 (2006).
[58] E. Ardonne, Phys. Rev. Lett. **102**, 180401 (2009).
[59] M. Greiter, Bull. Am. Phys. Soc. **38**, 137 (1993).
[60] A. Kumar, G. A. Csáthy, M. J. Manfra, L. N. Pfeiffer, and K. W. West, Phys. Rev. Lett. **105**, 246808 (2010).
[61] A. Kumar, N. Samkharadze, G. A. Csáthy, M. J. Manfra, L. N. Pfeiffer, and K. W. West, Phys. Rev. B **83**, 201305 (2011).
[62] Z. Liu *et al.*, in progress.
[63] S. Geraedts, M. P. Zaletel, Z. Papić, and R. S. K. Mong, Phys. Rev. B **91**, 205139 (2015).
[64] M. R. Peterson, Y.-L. Wu, M. Cheng, M. Barkeshli, Z. Wang, and S. Das Sarma, Phys. Rev. B **92**, 035103 (2015).
[65] W. Zhu, S. S. Gong, D. N. Sheng, and L. Sheng, Phys. Rev. B **91**, 245126 (2015).